THE JOURNAL OF PHYSICAL CHEMISTRY B
A JOURNAL OF THE AMERICAN CHEMICAL SOCIETY

pubs.acs.org/JPCB Article

OPLS/2020 Force Field for Unsaturated Hydrocarbons, Alcohols, and Ethers

Published as part of The Journal of Physical Chemistry B virtual special issue "Recent Advances in Simulation Software and Force Fields".

William L. Jorgensen,* Mohammad M. Ghahremanpour, Anastasia Saar, and Julian Tirado-Rives

Cite This: *J. Phys. Chem. B* 2024, 128, 250−262 Read Online

ACCESS | Metrics & More | Article Recommendations | Supporting Information

ABSTRACT: The OPLS all-atom force field was updated and applied to modeling unsaturated hydrocarbons, alcohols, and ethers. Testing has included gas-phase conformational energetics, properties of pure liquids, and free energies of hydration. Monte Carlo statistical mechanics (MC) calculations were used to model 60 liquids. In addition, a robust, automated procedure was devised to compute the free energies of hydration with high precision via free-energy perturbation (FEP) calculations using double annihilation. Testing has included larger molecules than in the past, and parameters are reported for the first time for some less common groups including alkynes, allenes, dienes, and acetals. The average errors in comparison with experimental data for the computed properties of the pure liquids were improved with the modified force field (OPLS/2020). For liquid densities and heats of vaporization, the average unsigned errors are 0.01 g/cm^3 and 0.2 kcal/mol. The average error and signed error for free energies of hydration are both 1.2 kcal/mol. As noted before, this reflects a systematic overestimate of the hydrophobicity of organic molecules when the parametrization is done to minimize the errors for properties of pure liquids. Implications for the modeling of biomolecular systems with standard force fields are considered.

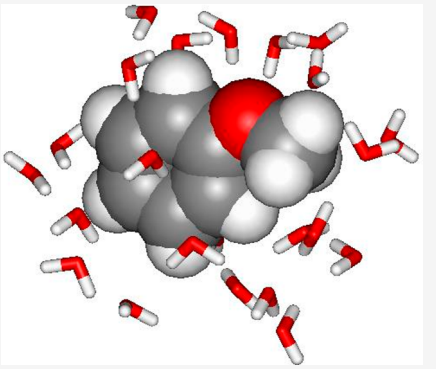

INTRODUCTION

Fixed-charge atomic force fields have been under development for more than 40 years, and they remain the mainstays of the description of energetics in condensed-phase simulations of organic and biomolecular systems.[1−5] Our group's early contributions in this area included the TIP3P and TIP4P water models[6] and the united-atom[7] and all-atom OPLS force fields.[8] Owing to implementation of simulations in the NPT ensemble in our Metropolis Monte Carlo code in 1981, it was possible to parametrize the force fields such that they could reproduce well not only gas-phase structures and energetics but also properties of liquids, especially densities and heats of vaporization. This required iterative simulations for numerous pure liquids, which was very demanding for computer resources at the time. Since then, there have been continual improvements in all the widely used force fields to increase their accuracy and scope, and in response to deficiencies that became apparent with applications to ever larger and more diverse systems.[4,5] For our OPLS force fields, improvements included better representation of torsional energetics for protein side chains[9] and treatment of halogen bonding[10] and cation−π interactions.[11] Most recently, alkanes were revisited to improve the thermodynamic results for long-chain alkanes and heats of vaporization for linear and branched isomers.[12] Twenty-five alkane liquids were modeled with monomers as large as hexadecane. Only six alkanes with no more than 6 carbon atoms were treated in the original OPLS-AA studies[8,13] with subsequent modeling of *n*-alkane liquids through dodecane.[14] The improved version of the force field is referred to as OPLS/2020.

In the present work, results of corresponding refinement and testing are reported for additional key classes of organic molecules, namely, unsaturated hydrocarbons, alcohols, and ethers. Again, a much broader range of systems is considered, including 60 liquids, and parameters are provided for the first time for alkynes, dienes, and allenes. A robust FEP-based protocol for computation of free energies of hydration is also reported, with results for 43 organic molecules.

The evolution of the OPLS all-atom force fields has been such that parametrization has occurred for many other systems too, but it has not been possible to formally present all the

Received: October 3, 2023
Revised: November 23, 2023
Accepted: November 28, 2023
Published: December 21, 2023

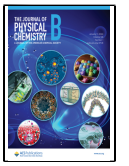

https://doi.org/10.1021/acs.jpcb.3c06602
J. Phys. Chem. B 2024, 128, 250−262

results. To help in this regard, the complete, current parameter files for the OPLS all-atom force field are provided in the Supporting Information. Access to the BOSS program, which uses the force field for a wide range of modeling applications including energy minimizations, conformational search, liquid simulations, FEP, and QM/MM calculations, is also freely available for these purposes as well as testing correct implementation of the force field in other software.

COMPUTATIONAL DETAILS

Pure Liquids. The calculations used the BOSS program, version 5.0.[15] All details for the Monte Carlo simulations of pure liquids were identical to those in the prior study of alkanes.[12] Key points are that the calculations are carried out for cubic samples of 500 molecules using periodic boundary conditions in the NPT ensemble at 25 °C and 1 atm, except as noted for low-boiling cases. Interactions between two molecules are truncated if no intermolecular distance between non-hydrogen atoms is less than 12 Å; quadratic smoothing is applied over the last 0.5 Å, and a standard correction for Lennard-Jones interactions neglected beyond the cutoff is included (eq 1). Here, i and j are the atoms in a monomer, N is the number of monomers, g_{ij} is the radial distribution function taken as 1 beyond the cutoff r_c, and u_{ij} is the Lennard-Jones potential.

$$E_c = (N/2) \sum_i \sum_j \int_{r_c}^{\infty} 4\pi r^2 \rho g_{ij}(r) u_{ij}(r)\, dr \quad (1)$$

For pure organic liquids such as the ones modeled here, there is no need for long-range corrections for the electrostatic (Coulomb) energy with reasonable cutoffs. There is sufficient disorder in the liquids that such corrections are negligible, as reflected in the fact that all radial distribution functions for a liquid such as ethanol have a value of 1.0 beyond 7.0 Å. To emphasize the point, MC simulations for ethanol were repeated twice with cutoffs of 8, 10, 12, and 14 Å in long simulations with 25×10^6 (25 M) configurations of equilibration starting from an already equilibrated configuration and averaging for another 50 M configurations. The average total intermolecular Coulomb energies for the 500 molecules were −3422, −3435, −3412, and −3411 kcal/mol, respectively, with average batch-mean uncertainties of ±7 kcal/mol. Thus, there is no statistically significant difference in the results for cutoffs of 8 Å or larger. Application of corrections such as Ewald for such systems seems worse than pointless since it introduces a nonphysical periodicity. On the other hand, there is need for the Lennard-Jones cutoff correction. For the 8, 10, 12, and 14 Å cutoffs, its values are −191, −98, −56, and −35 kcal/mol, respectively, out of a total intermolecular energy of ca. −4850 kcal/mol for N = 500.

All inter- and intramolecular degrees of freedom are sampled, and volume changes are attempted every 3125 configurations. Initial coordinates are generated by an algorithm that distributes monomers evenly in a box with a density of about 20% less than the estimated final density. Each liquid is equilibrated to convergence typically for at least 50 M configurations, and the subsequent averaging occurs over 25 M−50 M configurations. The equations used to evaluate properties of the liquids and the force field are the same as presented in ref 12. The nonbonded interactions are described using the Coulomb plus 12-6 Lennard-Jones form (eq 2). They are evaluated for all intermolecular pairs of atoms in molecules, a and b, and

$$E_{ab} = \sum_i^{\in a} \sum_j^{\in b} \left[\frac{q_i q_j}{r_{ij}} e^2 + 4\varepsilon_{ij} \left(\frac{\sigma_{ij}^{12}}{r_{ij}^{12}} - \frac{\sigma_{ij}^{6}}{r_{ij}^{6}} \right) \right] f_{ij} \quad (2)$$

intramolecular pairs separated by >3 bonds with f_{ij} = 1.0, while f_{ij} = 0.5 for all intramolecular pairs separated by 3 bonds. q_i and q_j are the partial charges on atoms i and j, which are separated by the distance r_{ij}. The combining rules for the Lennard-Jones parameters are $\sigma_{ij} = (\sigma_{ii}\sigma_{jj})^{1/2}$ and $\varepsilon_{ij} = (\varepsilon_{ii}\varepsilon_{jj})^{1/2}$.

Molecular dynamics simulations were also carried out using GROMACS (version 2019)[16] for 13 pure liquid alcohols and benzene analogues in order to compute diffusion constants in the same manner as described for alkanes.[12] Key details are that 512 molecules were used in a cubic cell with periodic boundary conditions along with a v-rescale thermostat and c-rescale barostat to maintain the temperature and pressure at 25 °C and 1 atm. The particle mesh Ewald algorithm was used for the long-range corrections, as this is the default setting, and the lengths of covalent bonds to hydrogen atoms were kept fixed. Each system was equilibrated for 2.5 ns, followed by averaging for 10 ns with a time step of 1 fs. Full details are provided in the Supporting Information.

Aqueous Solutions. Absolute free energies of hydration (ΔG_{aq}) were also computed with MC simulations by using free energy perturbation (FEP) theory. This was done by calculating the difference in free energy changes for disappearing the molecule of interest both in the gas-phase and in aqueous solution.[17−20] Separate simulations are run to remove the Coulomb and Lennard-Jones interactions. All aqueous simulations were performed using the *NPT* ensemble at 25 °C and 1 atm in a periodic cube, ca. 25 Å on an edge, containing 500 TIP4P water molecules.[21] All solvent−solvent and solute−solvent intermolecular interactions were truncated at 10 Å with quadratic smoothing over the last 0.5 Å and with a Lennard-Jones cutoff correction, as above. If any distance between non-hydrogen atoms in two molecules is less than the 10 Å cutoff, the entire molecule−molecule interaction is included. As above, a longer cutoff is unnecessary, and 12 Å is too close to the maximum of half the box edge given the volume fluctuations in *NPT* simulations. The ranges for variations of the solute and solvent molecules are chosen to give acceptance rates of 30−40% for new MC configurations.

A general protocol was optimized and implemented in the BOSS software. With a single command it takes the *Z*-matrix (internal coordinate representation with atom types)[16] for the molecule and sets up and executes the four MC simulations corresponding to turning off the Coulomb and Lennard-Jones interactions for the solute in both the gas phase and TIP4P water. The effects of the number of FEP windows with progress parameter λ and length of runs were studied. For molecules of the size considered here, it was found that 20 FEP windows with even spacing ($\Delta\lambda$ = 0.05) were adequate for all FEP calculations. The windows are run sequentially, with the last configuration serving as the starting point for equilibration in the next window.

For the gas-phase calculations, the equilibration and averaging periods are 0.1 and 2 M configurations, respectively, for each window. For the aqueous calculations, the MC calculations begin from a configuration generated by inserting the solute in an equilibrated box of 512 TIP4P water molecules

https://doi.org/10.1021/acs.jpcb.3c06602
J. Phys. Chem. B 2024, 128, 250−262

and automatically deleting the 12 water molecules with the most unfavorable interactions with the solute, leaving the solute and 500 water molecules. The partial charge removal then uses 3 M configurations of equilibration and 200 M configurations of averaging in each window with all other parameters unchanged. The end state for the removal of the Lennard-Jones interactions is the chargeless molecule with all bond length r_0 values reduced to 0.3 Å. In the absence of this shrinkage, numerical problems are encountered for larger solutes, owing to the resultant dispersed array of small Lennard-Jones particles. Importantly, the Lennard-Jones contribution is computed in the creation direction starting from the shrunken state and evolving to the full chargeless molecule.[22] Equilibration consists of 6 M configurations for the first window and 3 M configurations for subsequent windows. The averaging period is then 500 M configurations for each window. Thus, in all, the number of aqueous MC configurations is 4 billion for charge annihilation and 10 billion for Lennard-Jones change to obtain the absolute free energy of hydration for a molecule. On a 3 Gz processor, the times required are ca. 1 and 2.5 days. Of course, calculations for multiple molecules may be run simultaneously on multiprocessor systems.

The resultant uncertainty in the computed free energies of hydration was determined from independent calculations and from comparisons of results from the described protocol and earlier ones. In particular, results were obtained for many molecules with an alternative that used 12 windows for the aqueous calculations with 100 and 800 M configurations of averaging for the Coulomb and Lennard-Jones components. For example, the 12- and 20-window protocols gave the following results in kcal/mol for methanol (−4.612, −4.618), ethanol (−4.655, −4.608), butane (3.199, 3.139), and benzene (0.251, 0.200). The Lennard-Jones calculations for the 12-window calculations for butane were also extended with the following results for 800 M (3.199 kcal/mol), 1600 M (3.189), 2400 M (3.181), and 3200 M (3.168). Similar extension for pentane, hexane, heptane, and octane to 2400 M configurations also did not change the results by more than 0.06 kcal/mol. The 12- and 20-window protocols give equivalent results for the molecules and establish an uncertainty of ca. ±0.05 kcal/mol.

RESULTS

Force Field. The OPLS all-atom force fields use two-letter code XY for different atom types. Key examples are shown in Table 1, and the full list is provided in the Supporting Information. In order to represent diverse organic ions and molecules, an expanded set is used to include less common atom types such as C2 in allenes, N in azides, C2 and C3 in dienes and trienes, and atoms in 3- and 4-membered rings. The bond stretching, angle bending, and torsional parameters are then associated with doublets, triplets, and quartets of atom types; e.g., for methanol, there are CT-HC, CT-OH, and OH-HO bond stretching terms, HC-CT-HC, HC-CT-OH, and CT-OH-HO angle bending terms, and the single HC-CT-OH-HO torsion term. The complete listing of parameters is provided in two files, *oplsaa.par* for the nonbonded (q, σ, ϵ) and torsional parameters and *oplsaa.sb* for the bond stretching and angle bending parameters. The coverage for bond stretching and angle bending is extensive; therefore, missing parameters are not common. Parameters for more than 1200 torsion types are also provided; however, for complex polyfunctional molecules, some torsion types may be missing. In all cases, when using the BOSS program,[15] if a parameter is missing, a hierarchy of procedures is used to estimate it starting first with the use of synonyms; e.g., for quinoline, if CB-NC was missing, CA-NC could be used. In addition, some atom types have been explicitly added to improve the torsional energetics; e.g., for biaryl systems like biphenyl, the use of CA-C!-C!-CA terms for the biaryl junction is needed to be distinguished from CA-CA-CA-CA, which would force planarity.[23] Similarly, the carbon atoms in alkenes, dienes, and trienes are declared as CM-CM, CM-C=-C=CM, and CM-C=-C#-C#-C=-CM to yield proper structures and torsional energetics. Treatment of larger polyenes requires a perception algorithm to assign the parameters to generate the structures with alternating double and single bonds.

Table 1. Partial List of Two-Letter Atom Types for OPLS Force Fields

Code	Description	Code	Description
C	carbonyl C	H	amide, amine, or silane H
CT	alkane C	HC	alkane, alkene, alkyne H
CM	alkene C	HA	benzene-like H
CA	aromatic C in 6-ring	HO	alcohol H
CB	aromatic fusion C as in naphthalene	HS	thiol H
CO	acetal C (O- CR2 -O)	O	carbonyl O
C=	C2 in dienes (C1 is CM)	OH	alcohol O
C#	C3 in trienes (C1 is CM, C2 is C=)	OS	ether O
C:	allene and ketene C2	ON	O in N=O
CZ	sp C in triple bond	OY	O in S=O
C+	carbenium carbon	O$	O in 3-ring or 4-ring, e.g., epoxide
C!	C1 in biphenyl-like ring	OA	O in furan, oxazole, etc.
CW	C2 in aromatic 5-ring like furan	N	amide N
CP	C2 in thiophene	NM	N in tertiary amide
CS	C3 in aromatic 5-ring like furan	NA	5- or 6-ring aryl N-H
CV	C4 in aromatic like oxazole, imidazole	NB	N= in 5-ring like oxazole, imidazole
CU	C5 in aromatic like pyrazole, isoxazole	NC	pyridine N
CX	C=C in protonated imidazole, histidine	NH	N-H as in pyrrole
CY	sp^3 carbon in 3-ring or 4-ring	NS	N-alkyl in pyrrole
C$	carbonyl C in 3-ring or 4-ring	NX	N-aryl in pyrrole
CF	carbon in perfluoroalkane	N$	N in 3-ring or 4-ring, e.g., aziridine
S	S in sulfide	NT	N in amine
SH	S in thiol	NZ	sp N in nitrile or azide
SY	S in sulfonamide or sulfone	N=	N2 in azadiene C=N-C=C
SZ	S in sulfoxide	NO	N in nitro, nitroso
S=	S in thiocarbonyl like thiourea	Si	Si in silane
P	P in phosphate		

For the present study, OPLS all-atom parameters were tested and refined for unsaturated hydrocarbons, alcohols, and ethers. The parametrization, as usual, emphasized gas-phase structures, conformational energetics, and pure liquid densities and heats of vaporization. The prior reported work with OPLS-AA for liquids was limited in scope, only covering propene, (*E*)-but-2-ene, benzene, halobenzenes,[10] methanol, ethanol, propanol, isopropanol, *t*-butanol, phenol, methyl ether, ethyl methyl ether, ethyl ether, tetrahydrofuran, dimethoxymethane, and 1,3-dioxolane.[8] This has been expanded to 60 liquids here

https://doi.org/10.1021/acs.jpcb.3c06602
J. Phys. Chem. B 2024, 128, 250−262

with the treatment of much larger and more branched molecules. The resultant nonbonded parameters for hydrocarbons and aryl halides are provided in Table 2, and those for alcohols and ethers are listed in Table 3 with new values in bold. The bond stretching, angle bending, and torsional parameters are listed in the Supporting Information. It may be noted that parameters for alkynes, allenes, polyenes, polyols, and vinyl ethers have not been reported previously, though earlier versions have been available on request and through distribution of the BOSS program.

Table 2. OPLS All-Atom Non-Bonded Parameters for Hydrocarbons and Aryl Halides[a]

Atom	Type	OPLS-2020 q	σ	ε
Alkanes[b]				
n-CH_3	CT	−0.18	3.550	0.066
iso-CH_3	CT	−0.18	3.400	0.072
neo-CH_3	CT	−0.18	3.340	0.070
CH_2	CT	−0.12	3.510	0.066
CH	CT	−0.06	3.500	0.066
C	CT	0.00	3.500	0.066
CH_2 in c-C3	CY	−0.12	3.430	0.088
CH_2 in c-C4	CY	−0.12	3.470	0.077
H in alkane	HC	0.060	2.480	0.026
Arenes				
C in benzene	CA	−0.115	3.550	**0.068**
C1 in Ph-Ph	C!	0.00	3.550	**0.068**
C9 in naphthalene	CB	0.00	**3.550**	**0.068**
H in PhH	HA	0.115	2.420	0.030
C in $PhCH_3$	CT	−0.065	**3.550**	0.066
C in $PhCH_2R$	CT	−0.005	**3.510**	**0.066**
C in $PhCHR_2$	CT	0.055	**3.500**	**0.066**
C in $PhCR_3$	CT	0.115	**3.500**	**0.066**
Aryl Halides				
F in PhF	F	**−0.280**	2.850	0.061
Cl in PhCl	Cl	−0.180	3.400	0.300
Br in PhBr	Br	**−0.150**	3.470	**0.450**
I in PhI	I	−0.100	**3.800**	**0.580**
Cipso in PhX	CA	−qX	3.550	**0.068**
F in PhF2	F	−0.200	2.850	0.061
F in C6F6	F	−0.130	2.850	0.061
Alkene, Diene				
C in $=CH_2$	CM	−0.230	3.550	0.076
C in =CHR	CM	−0.115	3.550	0.076
C in $=CR_2$	CM	0.0	3.550	0.076
H in =CH	HC	0.115	2.420	0.030
C2 in C=CH-C=C	C=	**0.115**	**3.550**	**0.076**
C2 in C=CR-C=C	C=	**0.000**	**3.550**	**0.076**
Allene				
=C=	C:	**−0.100**	**3.300**	**0.086**
$=CH_2$	CM	**−0.250**	**3.300**	**0.086**
=CHR	CM	**−0.100**	**3.300**	**0.086**
$=CR_2$	CM	**0.050**	**3.300**	**0.086**
H in =C=CHR	HC	**0.150**	**2.420**	**0.030**
Alkyne				
C in ≡C	CZ	**−0.200**	**3.500**	**0.110**
H in ≡CH	HC	**0.200**	**2.420**	**0.015**
C3 in H_3C-C≡C	CT	**0.020**	**3.550**	**0.066**
C3 in RH_2C-C≡C	CT	**0.080**	**3.510**	**0.066**
C3 in R_2HC-C≡C	CT	**0.140**	**3.500**	**0.066**
C3 in R_3C-C≡C	CT	**0.200**	**3.500**	**0.066**

[a]Lennard-Jones σ in Å; ε in kcal/mol. $R^* = 2^{1/6}(\sigma/2)$. Values in bold are new. [b]Ref 13.

Table 3. OPLS All-Atom Non-Bonded Parameters for Alcohols and Ethers[a]

Atom	Type	OPLS-2020 q	σ	ε
Alcohols				
O in 1°, 2° ROH	OH	−0.683	3.120	0.170
O in 3° ROH	OH	**−0.650**	**3.120**	**0.170**
H_O in ROH	HO	0.418	0.0	0.0
C_O in 1° ROH	CT	0.145	3.500	0.066
C_O in 2° ROH	CT	0.205	3.500	0.066
C_O in 3° ROH	CT	**0.232**	3.500	0.066
H_C in CH_3OH	HC	0.040	2.500	0.030
H_C in RCH_nOH	HC	0.060	2.480	0.026
O in PhOH	OH	**−0.530**	3.070	0.170
H_O in PhOH	HO	**0.430**	0.0	0.0
C_O in PhOH	CA	**0.100**	3.550	0.070
O in 1,2-diol	OH	**−0.700**	3.070	0.170
H_O in 1,2-diol	HO	**0.435**	0.0	0.0
O in 1,2,3-triol	OH	**−0.730**	3.070	0.170
H_O in 1,2,3-triol	HO	**0.465**	0.0	0.0
C_O 1° diol and triol	CT	**0.145**	3.510	0.066
C_O 2° diol and triol	CT	**0.205**	3.500	0.066
C_O 3° diol and triol	CT	**0.265**	3.500	0.066
Ethers				
O in ROR	OS	−0.400	2.900	**0.120**
O in PhOR	OS	**−0.285**	**2.900**	**0.140**
O in PhOPh	OS	**−0.170**	**2.900**	**0.140**
C_O in CH_3OR	CT	0.110	3.500	0.066
C_O in RCH_2OR	CT	0.140	3.500	0.066
C_O in R_2CHOR	CT	0.170	3.500	0.066
C_O in R_3COR	CT	0.200	3.500	0.066
C_{ipso} in PhOR	CA	**0.085**	**3.550**	**0.068**
alpha H in ROR	HC	0.030	**2.480**	**0.026**
C_O in $ROCH{=}CR_2$	CM	**−0.030**	**3.550**	**0.076**
C_O in $ROCR{=}CR_2$	CM	**0.085**	**3.550**	**0.076**
O in acetal	OS	**−0.330**	2.900	0.140
C_O in $ROCH_2OR$	CT	**0.060**	3.500	0.066
C_O in ROCHROR	CT	**0.160**	3.500	0.066
C_O in $ROCR_2OR$	CT	**0.260**	3.500	0.066
H_C in ROCHROR	HC	**0.100**	2.500	0.030

[a]Lennard-Jones σ in Å; ε in kcal/mol. $R^* = 2^{1/6}(\sigma/2)$. Values in bold are new.

Conformational Energetics. Results for the relative conformational energies of prototypical molecules from the force field are compared in Table 4 with literature results of high-level ab initio quantum mechanical (QM) calculations and experimental data.[23−39] The QM calculations typically included the correlation energy at least at the MP2 level and used double- or triple-ζ basis sets with polarization functions. Overall, the agreement between the QM and force field results is generally within a few tenths of a kcal/mol.

Several cases warrant more comment. For 1-butene, the C-C-C-C *skew* − *cis* difference is computed to be 0.2 kcal/mol higher than the experimental value with the force field, while it is underestimated by 0.3 kcal/mol using MP4SDQ calculations.[24] For the isoelectronic methyl vinyl ether, the force field and experiment disfavor the *skew* form by 1.7 kcal/mol, while the MP4SDQ result is higher at 2.3 kcal/mol. The *E*/*Z*

https://doi.org/10.1021/acs.jpcb.3c06602
J. Phys. Chem. B 2024, 128, 250−262

Table 4. Relative Gas-Phase Conformational Energies (kcal/mol)

Molecule	Conformers	QM	Expt	OPLS/2020
1-butene	skew−cis	0.26[a]	0.53[a]	0.75
2-butene	*Z*−*E*	1.27[a]	1.0[a]	0.87
cyclooctene	*E*−*Z*	8.14[b]	11.37[c]	14.43
ethene	perp−plnr	65.4[d]	65[d]	69.91
1,3-butadiene	skew−a	2.39[a]	2.49[a]	2.60
styrene	plnr−twist	0.24[e]		0.04
styrene	perp−twist	2.74[e]	3.0−3.4[e]	3.24
toluene	90°−0°	0.06		0.13
ethylbenzene	plnr−perp	1.39[f]	1.18[f]	1.46
biphenyl	plnr−twst	2.1[g]	1.4 ± 0.5[g]	2.30
methanol	ecl−stag	1.02[h]	1.07[h]	1.07
ethanol	g−a	0.12[h]	0.12[h]	0.27
propanol	aa−ga	0.17[h]		0.33
isopropanol	a−g	0.26[h]	0.28[a]	0.26
ethane-1,2-diol	ggg^+−agg^+	0.46[i]		0.31
ethane-1,2-diol	aaa−agg^+	2.07[i]		1.98
phenol	perp−plnr	3.58[j]	3.47[j]	3.46
anisole	perp−plnr	2.48[j]	<3.1[j]	2.96
ethyl methyl ether	g−a	1.32[k]	1.5[a]	1.24
ethyl ether	ag−aa	1.29[k]	1.1[a]	1.28
ethyl ether	g^+g^+−aa	2.48[k]		2.56
methyl propyl ether	aa−ga	0.36[l]		0.03
methyl propyl ether	g^+g^+−ga	1.28[l]		1.16
methyl propyl ether	ag−ga	1.74[l]		1.25
methyl vinyl ether	skew−cis	2.27[a]	1.7[a]	1.71
methoxycyclohexane	ax−eq	0.01[a]	0.45[a]	0.51
1,2-dimethoxymethane	ag^+- g^+g^+	2.54[m]		2.09
1,2-dimethoxymethane	aa−g^+g^+	5.55[m]		4.41
2-methoxy-THP	eq−ax	1.42[n]	1.21[o]	0.71
1,2-dimethoxyethane	aga−aaa	0.38[p]		0.53
1,2-dimethoxyethane	aag−aaa	1.44[p]		1.30
18-crown-6	C_i−S_6	0.2[q]		1.01
18-crown-6	D_{3d}−S_6	4.3[q]		6.01
18-crown-6	D_2−S_6	5.0[q]		5.18

[a]Ref 24. [b]Ref 25. [c]Ref 26. [d]Ref 27. [e]Ref 28. [f]Ref 29. [g]Ref 23. [h]Ref 30. [i]Ref 31. [j]Ref 32. [k]Ref 33. [l]Ref 34. [m]Ref 35. [n]Ref 36. [o]Ref 37. [p]Ref 38. [q]Ref 39.

energy difference for 2-butene and rotational barrier for ethene are well reproduced by the force field, while the experimental value for the *E*/*Z* difference for cyclooctene lies between the results from the force field and G3(MP2) calculations.[25,26] The latter system was not considered during the parametrization; some adjustment of angle-bending parameters could be tested.

The *skew* form for 1,3-butadiene is also disfavored relative to the *anti* conformer, with good agreement between the computed and experimental values of ca. 2.5 kcal/mol. Even higher-level CCSD(T) calculations for 1,3-butadiene yield a *skew* − *anti* difference of 2.9 kcal/mol, a *skew* to *cis* barrier of 0.3 kcal/mol, an *anti* to *skew* barrier of 5.7 kcal/mol, and dihedral angles of 36° for skew and 102° for the latter transition state.[40] The corresponding values from the force field are 2.6, 0.2, and 4.8 kcal/mol with dihedral angles of 30° and 100°. In the phenyl analogue, styrene, there are four shallow minima with CCCC dihedral angles of ca. ±20° and barriers to planarity of only 0.04 kcal/mol from the force field or 0.24 kcal/mol from MP2/6-31G(d) calculations.[28] The deconjugated, perpendicular rotamers are transition states, 3.2 kcal/mol above the minima from both the force field and experiments. Figure 1 shows the full torsional profiles for several prototypical hydrocarbons from the force field, with results in close agreement with the cited quantum mechanical studies.

For the substituted benzenes, phenol, anisole, and ethylbenzene (Figure 1), the force field gives results very close to the experimental values and correctly prefers planar structures for the two former substituted molecules and a perpendicular geometry for the latter. For ethyl methyl ether and diethyl ether, the single *gauche* conformer lies 1.2−1.3 kcal/mol above the *anti* conformer from the force field and MP2/6-31G(d,p) optimizations,[34] while the experimental values are 1.1−1.5 kcal/mol. These values are significantly higher than the *gauche* − *anti* difference for butane (Figure 1) and pentane[12] of 0.5−0.6 kcal/mol owing to the shorter C-O bonds in ethers than C-C bonds in alkanes, which leads to closer C1-C4 *gauche* contact in ethers.

1,2-Dimethoxymethane is a prototypical system for the anomeric effect yielding a 2.1−2.5 kcal/mol preference for the *gauche*$^+$-*gauche*$^+$ conformer or its enantiomer over *anti*-*gauche*.[35] Analogously, the axial conformer of 2-methoxytetrahydropyran is favored over the equatorial conformer by 0.71 kcal/mol using the force field. Ab initio results for this system are sensitive to the basis set and treatment of the correlation energy with the best CCSD(T) results predicting 1.42 kcal/

https://doi.org/10.1021/acs.jpcb.3c06602
J. Phys. Chem. B 2024, 128, 250−262

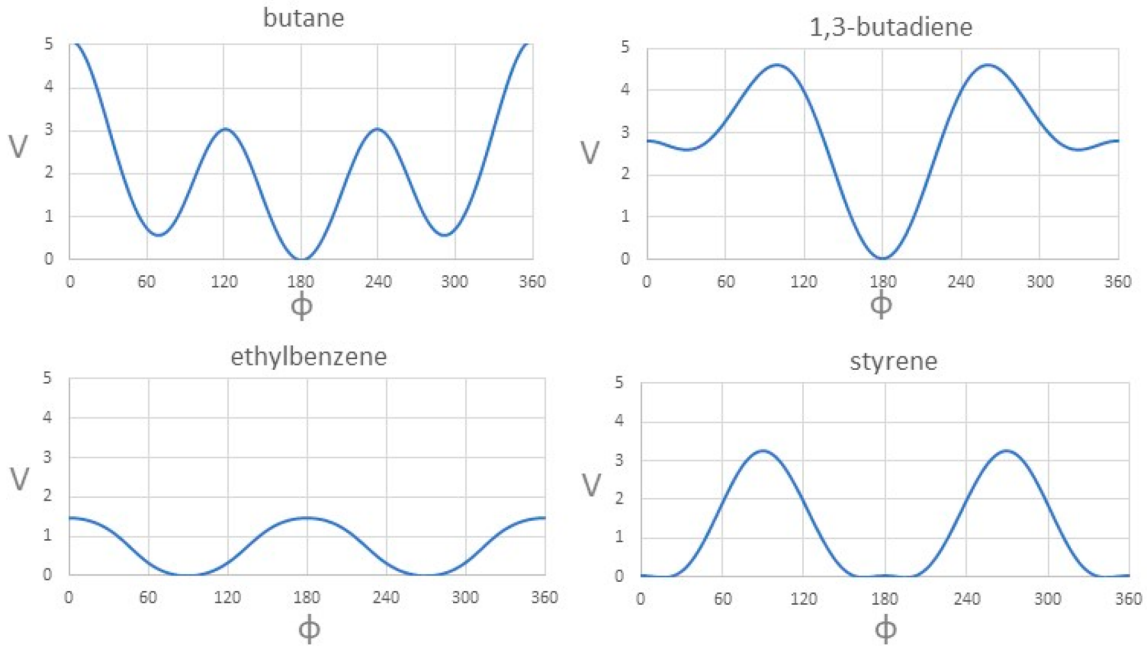

Figure 1. Torsional energy profiles for rotation about the central CC single bonds in butane, 1,3-butadiene, ethylbenzene, and styrene, from the OPLS/2020 force field. Potential energy in kcal/mol; dihedral angle in degrees.

mol,[36] while the thermochemical measurements of Wiberg and Marquez gave 1.21 ± 0.07 kcal/mol.[37] There are substantial solvent effects in this case with the equatorial form becoming favored in aqueous solution.[37,41]

Finally, the *aga* conformer of 1,2-dimethoxyethane with the O-C-C-O angle *gauche* is computed with the force field to be 0.53 kcal/mol higher in energy than the all-*anti* conformer, which can be compared with MP3, MP4(SDQ), and MP4(SDTQ) values of 0.64, 0.55, and 0.38 kcal/mol, respectively.[38] A challenging test of the OS-CT-CT-OS, CT-CT-OS-CT, and nonbonded parametrization was then carried out through a conformational search for 18-crown-6. Sharapa et al. have reported DLPNO-CCSD(T) results as a reference and focused on the relative energies of the S_6 (global minimum), D_{3d} (crown), and D_2 conformers, as illustrated in Figure 2.[39] The agreement between the results from the

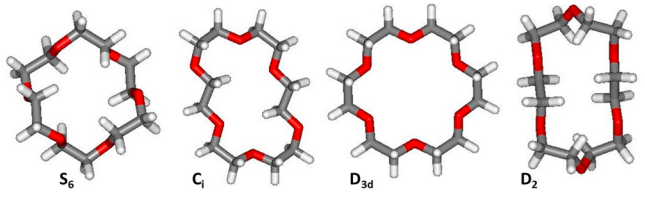

Figure 2. Structures of four conformers of 18-crown-6 as optimized with OPLS/2020.

present OPLS/2020 force field and the reference data is strikingly good compared with the predictions from a wide variety of semiempirical QM and DFT-based methods. For example, in comparison to the average differences of 1 kcal/mol with OPLS/2020 in Table 4, PM6, PM7, DFTB3, and GFN2-xTB give discrepancies averaging 32, 21, 5, and 14 kcal/mol, respectively.[39] The average errors with the MMFF94 and MM3 force fields were also reported as 6 and 13 kcal/mol.[39] In addition, Sharapa et al. found that a C_i conformer is second-lowest in energy, just 0.2 kcal/mol above S_6; the OPLS/2020 force field gives a difference of 1.0 kcal/mol. An extensive conformational search with OPLS/2020 did not yield any conformers lower in energy than the S_6 one.

Pure Liquids. The computed and experimental densities and heats of vaporization for the 23 unsaturated hydrocarbons and aryl halides are compared in Table 5. The corresponding results for 37 polar liquids, including alcohols, ethers, and polyols, are listed in Table 6. The results for the 60 liquids are combined and plotted in Figure 3. The average errors are 0.01 g cm^{-3} for the densities and 0.2−0.3 kcal/mol for the heats of vaporization, and the correlation coefficients r^2 are 0.99 for the plots in Figure 3. The accuracy is similar to that for alkanes.[12] The testing is much greater than in the past, including more branched and larger molecules. From independent calculations the uncertainties in the computed densities range from ±0.001 g cm^{-3} for the smaller molecules to ±0.01 g cm^{-3} for the largest ones; the corresponding uncertainties for ΔH_{vap} are ±0.03 to ±0.2 kcal/mol. The equilibration for octanol was carefully studied and showed good convergence (±0.2% for the density and ±1% for the energy) after 200 M configurations.

For alkylbenzenes, the only changes in parameters were to adopt the new Lennard-Jones parameters for alkyl groups[12] and to change the ε for benzene carbon atoms to 0.068 kal/mol from 0.070 kcal/mol.[8,44] This small change has little effect on the computed densities for benzene through *t*-butylbenzene; however, it lowers the computed heats of vaporization by 0.2−0.3 kcal/mol, which lowers the average error by ca. 2%. It does worsen a little the results for liquid benzene. The original parametrization with the present MC protocol gives a density and ΔH_{vap} of 0.872 g cm^{-3} and 8.077 kcal/mol, while the present results are 0.863 g cm^{-3} and 7.827 kcal/mol and the experimental values are 0.874 g cm^{-3} and 8.090 kcal/mol. It may be noted that results were first reported with the original parametrization in 1990 with a smaller system size (128 monomers), much shorter averaging (3.5 M configurations), a 13 Å ring center−ring center cutoff, rigid vs flexible monomers,

https://doi.org/10.1021/acs.jpcb.3c06602
J. Phys. Chem. B 2024, 128, 250−262

Table 5. OPLS/2020 Densities (g/cm^3) and Heats of Vaporization (kcal/mol) of Arene, Alkene, Alkyne, and Aryl Halide Liquids at 25 °C and 1 atm

Molecule	d(OPLS)	d(exptl)[a]	ΔH_{vap}(OPLS)	ΔH_{vap}(exptl)[a]
benzene	0.8634	0.8736	7.827	8.090
toluene	0.8621	0.8622	9.116	9.080
ethylbenzene	0.8590	0.8625	10.098	10.098
isopropylbenzene	0.8717	0.8574	10.997	10.789
t-butylbenzene	0.8879	0.8624	11.881	11.730
o-xylene	0.8730	0.8759	10.531	10.381
m-xylene	0.8632	0.8601	10.522	10.195
p-xylene	0.8620	0.8566	10.432	10.128
mesitylene	0.8681	0.8611	11.960	11.348
1-methylnaphthalene	1.0126	1.0168	14.690	14.357
phenylcyclohexane	0.9352	0.9387	14.583	14.330
1-pentene	0.6334	0.6353	6.069	6.088
(*Z*)-2-pentene	0.6381	0.6504	6.236	6.41
(*E*)-2-pentene	0.6331	0.6431	6.280	6.38
cyclohexene	0.7895	0.8061	7.750	7.922
styrene	0.9051	0.9012	10.524	10.500
1-butyne (T = 0 °C)	0.6622	0.6778[b]	5.851	6.000[b]
2-butyne (T = 0 °C)	0.6942	0.7119[b]	6.955	6.640[b]
fluorobenzene	1.0051	1.0190	8.255	8.260
chlorobenzene	1.0980	1.1009	9.696	9.792
bromobenzene	1.5230	1.4882	10.730	10.650
iodobenzene	1.8695	1.8229	11.725	11.850
hexafluorobenzene	1.5753	1.6073	8.690	8.530
mean % error	1.246		1.867	
mean unsigned error	0.013		0.176	

[a]Ref 42. [b]Ref 43.

and the same treatment of the Lennard-Jones interactions beyond the cutoff; the reported results for the density (0.873 ± 0.001 g cm^{-3}) and ΔH_{vap} (8.05 ± 0.01 kcal/mol) are essentially identical to those obtained here.[44]

The orderings of the computed and experimental results in Table 5 also agree well, for example, for the isomeric xylenes and mesitylene. With no further modification of parameters, it was gratifying that increased errors were not obtained for the larger 1-methylnaphthalene and phenylcyclohexane. The former liquid was modeled rather than naphthalene owing to their respective melting points of −30 and 80 °C.[42] Five liquid alkenes as large as styrene were modeled, with no anomalous results. Thermodynamic data on liquid alkynes is less common so only 1-butyne and 2-butyne were simulated at 0 °C. The four halobenzenes and hexafluorobenzene were also reconsidered in the all-atom format without additional X-sites for halogen bonding.[10] Some small adjustments were made to the nonbonded parameters, and it is noted that the magnitude of the charge on fluorine needs to decrease for polyfluorinated benzenes (Table 2). If consideration of halogen bonding is desired for X = Cl, Br, and I, the prescription provided previously can be followed.[10]

Turning to the alcohols in Table 6, the errors in computed densities remain around 0.01 g cm^{-3}, while typical errors for ΔH_{vap} are 0.3 kcal/mol, with a few cases of 0.5 kcal/mol or more. Glycerol could be expected to be challenging; indeed, the computed (22.5 kcal/mol) and experimental (21.9 kcal/mol) values differ by 0.6 kcal/mol or 2.6%. The discrepancies for 1,2-ethanediol, benzyl alcohol, and phenol are only 0.2−0.3 kcal/mol. However, *m*-cresol has a higher error (0.6 kcal/mol) for no obvious reason, though the pattern for toluene and *m*-xylene in Table 5 is similar, with a 0.3 kcal/mol greater error for the latter. The results for the *n*-alkanols, methanol through octanol, are uniformly good, which confirms the transferability of the parameters for alkanes.[12] The three secondary alcohols, 2-propanol, 2-butanol, and 3-pentanol, gave typical errors, although the 0.03 g cm^{-3} error in the density of 2-propanol is among the highest and goes along with the overestimate of its ΔH_{vap} by 0.3 kcal/mol. For tertiary alcohols (2-methyl-2-propanol and 2-methyl-2-butanol) it was found that the magnitude of the negative charge on oxygen had to be reduced by 0.03 e (Table 3) to avoid an overestimate of ΔH_{vap} values. A final point for the monoalcohols is that it is straightforward to obtain an accurate estimate of the number of hydrogen bonds per monomer from integration of the O-H radial distribution functions to the sharp minima that occur at 2.6 Å.[45] The present results are 1.88−1.96 for the primary alkyl alcohols, 1.70−1.89 for the secondary ones, and 1.60−1.73 for the tertiary alcohols, which reflects the expected steric effects with increasing substitution.[45] Phenol and *m*-cresol both show 1.6 hydrogen bonds per molecule, as before.[46]

Ten simple ethers were modeled along with the acetal dimethoxymethane, two 1,2-dialkoxyethanes, and 2-ethoxyethanol. There are no striking anomalies, though it is surprising that the computed heats of vaporization for THF and THP are within 0.1 kcal/mol, while they differ experimentally by 0.7 kcal/mol and the pattern for ethyl ether vs propyl ether was well reproduced. Results for propylamine, diethylamine, and triethylamine are also included in Table 6 to illustrate that the OPLS/2020 parameters for alkyl groups also merge well with the previously reported all-atom parameters for amines.[47]

Some additional results from the MC simulations for heat capacities and isothermal compressibilities are listed in Table 7. These quantities converge much more slowly than those for

https://doi.org/10.1021/acs.jpcb.3c06602
J. Phys. Chem. B 2024, 128, 250−262

Table 6. OPLS/2020 Densities (g/cm^3) and Heats of Vaporization (kcal/mol) of Polar Liquids at 25 °C and 1 atm

Molecule	d(OPLS)	d(exptl)[a]	ΔH_{vap}(OPLS)	ΔH_{vap}(exptl)[a]
methanol	0.7833	0.7864	8.996	8.91
ethanol	0.7958	0.7849	10.192	10.11
1-propanol	0.7980	0.7996	10.892	11.31
2-propanol	0.8135	0.7813	11.111	10.81
butanol	0.8002	0.8057	12.148	12.5
2-methyl-1-propanol	0.8175	0.7978	11.253	12.14
2-butanol	0.8179	0.8024	11.784	11.87
2-methyl-2-propanol	0.8147	0.7812	11.209	11.14
1-pentanol	0.8097	0.8108	13.341	13.61
3-methyl-1-butanol	0.8186	0.8071	13.280	13.0
3-pentanol	0.8132	0.8160	12.275	12.7
2-methyl-2-butanol	0.8233	0.8050	11.674	12.0
hexanol	0.8139	0.8153	14.843	14.73
2-ethyl-1-butanol	0.8253	0.8293	13.792	14.41
octanol	0.8156	0.8216	17.116	16.96
benzyl alcohol	1.0392	1.0413	15.909	15.71
1,2-ethanediol	1.0988	1.1100	16.473	16.20
glycerol	1.2088	1.2559	22.488	21.92
phenol	1.0653	1.0580	14.036	13.82
m-cresol	1.0281	1.0302	15.355	14.75
dimethyl ether (−24.84 °C)	0.7117	0.7262	5.068	5.143
ethyl ether	0.6973	0.70782	6.384	6.510
propyl ether	0.7317	0.7419	8.357	8.530
isopropyl ether	0.7413	0.71854	7.858	7.650
butyl ether	0.7596	0.7641	10.796	10.600
anisole	0.9699	0.9893	11.010	11.200
phenetole PhOEt	0.9541	0.9605	12.170	12.200
diphenyl ether	1.0633	1.071	16.469	15.990
tetrahydropyran THF	0.8466	0.8811	7.911	7.650
tetrahydropyran THP	0.8623	0.8772	7.975	8.350
dimethoxymethane	0.8463	0.8538	7.107	6.904
1,2-dimethoxyethane	0.8523	0.8637	9.059	8.697
1,2-diethoxyethane	0.8361	0.8351	10.544	10.330
2-ethoxyethanol	0.9027	0.9252	11.023	11.520
propylamine	0.7202	0.7121	7.811	7.471
diethylamine	0.7102	0.7016	7.702	7.486
triethylamine	0.7313	0.7231	8.546	8.320
mean % error	1.425		2.529	
mean unsigned error	0.012		0.284	

[a]Ref 42.

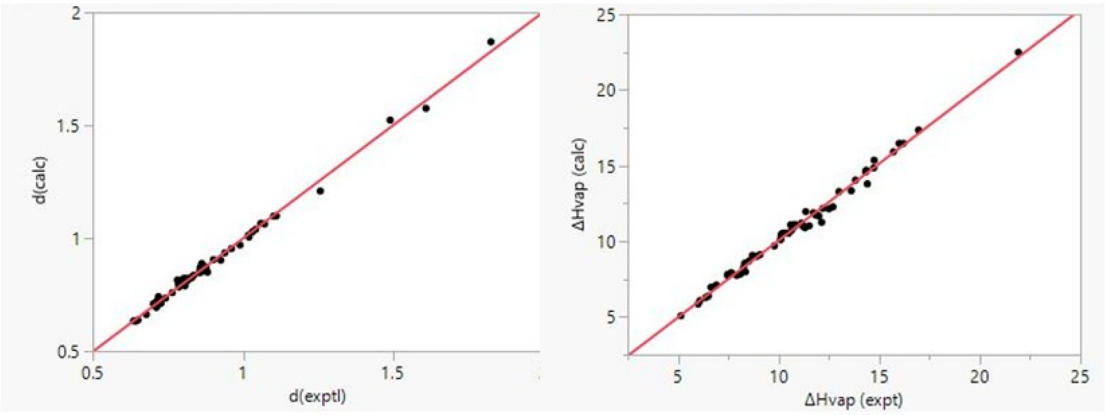

Figure 3. Comparison of computed OPLS/2020 and experimental densities and heats of vaporization.

the density and ΔH_{vap}, so the uncertainties are much greater. There is also relatively little experimental data available for compressibilities of organic liquids. For liquid hexane, perfect agreement was found between the values computed with the

https://doi.org/10.1021/acs.jpcb.3c06602
J. Phys. Chem. B 2024, 128, 250−262

Table 7. OPLS/2020 and Experimental Heat Capacities (cal mol^{-1} deg^{-1}) and Isothermal Compressibility Coefficients (atm^{-1}) for Liquids at 25 C and 1 atm[a]

Liquid	C_p°	Calc C_p(l)	Exp C_p(l)	Calc 10^6 κ	Exp 10^6 κ
benzene	19.52	34.9 ± 0.2	32.45	101.5 ± 11.6	97.9
toluene	24.80	41.4 ± 2.9	37.59	103.7 ± 13.4	92.3
ethylbenzene	30.69	44.3 ± 1.6	44.35	73.3 ± 8.0	87.6
cyclohexene	25.10	42.0 ± 3.1	34.7	139.3 ± 20.3	101.5
p-xylene	30.02	45.3 ± 1.6	43.42	73.2 ± 5.4	87.0
chlorobenzene	23.42	37.2 ± 1.2	35.57	80.4 ± 4.8	78.1
methanol	10.53	26.2 ± 1.1	19.47	80.5 ± 6.0	126.4
ethanol	15.64	34.8 ± 1.7	26.85	107.0 ± 9.4	116.8
butanol	26.29	54.8 ± 4.5	42.32	97.6 ± 12.5	95.4
hexanol	37.2	60.0 ± 3.9	57.68	81.1 ± 12.3	83.5
octanol	48.2	73.1 ± 3.7	73.03	58.8 ± 8.6	77.4
m-cresol	29.80	41.6 ± 0.8	53.76	34.8 ± 2.0	
ethyl ether	28.45	44.3 ± 1.6	41.23	244.2 ± 28.1	
propyl ether	38.0	51.5 ± 1.6	52.96	134.7 ± 14.6	155.1[c]
isopropyl ether	(38.0)	61.7 ± 3.3	51.65	216.8 ± 28.5	188.0[c]
anisole	31.1	46.4 ± 1.5	45.7	68.1 ± 5.9	
tetrahydrofuran THF	18.22	31.4 ± 1.3	29.61	118.0 ± 9.2	
2-ethoxyethanol	29.5	48.0 ± 2.2	50.38	79.2 ± 8.4	
propylamine	21.8	42.3 ± 3.0	38.84	196.1 ± 40.1	
diethylamine	27.1	49.0 ± 4.0	42.24	179.1 ± 22.9	
triethylamine	37.8	58.1 ± 3.0	53.40	168.3 ± 23.5	
mean % error		11.6		14.7[b]	
mean unsigned error		4.4		16.3[b]	

[a]Experimental data from ref 42. [b]Using 13 values. [c]Ref 48.

present force field and the experimental densities from 1 to 5000 atm at 25 °C.[12] There is also good agreement between the computed and experimental isothermal compressibilities in Table 7 in view of the computed uncertainties. The computed heat capacities in Table 7 are mostly a little greater than the experimental ones and give an average error of 4.4 ± 2.3 cal/(mol K). This seems acceptable, and it is unclear what modifications could be made to the force field for improvement.

The computed diffusion coefficients from the MD simulations are compared with the experimental data in Table 8, and the results for *n*-alcohols are also shown in Figure 4. The quality of the results is similar for the alcohols and

Table 8. Self-Diffusion Coefficients D_0 (10^{-5} cm^2 s^{-1}) of Liquids[a]

Molecule	Exptl.	OPLS/2020
methanol	2.27,[b] 2.44[c]	2.85 ± 0.10
ethanol	1.01,[b] 1.16,[c] 1.08[d]	1.34 ± 0.08
propanol	0.646,[b] 0.590,[c] 0.627[d]	0.85 ± 0.04
butanol	0.504,[b] 0.426,[e] 0.456[d]	0.60 ± 0.01
pentanol	0.296,[f] 0.286[g]	0.42 ± 0.01
hexanol	0.218[f]	0.28 ± 0.01
heptanol	0.172[f]	0.20 ± 0.01
octanol	0.138,[e] 0.142[f]	0.14 ± 0.01
2-propanol	0.649,[b] 0.582[c]	0.75 ± 0.03
benzene	2.25[h]	1.97 ± 0.14
toluene	2.40[h]	1.69 ± 0.08
ethylbenzene	1.98[i]	1.36 ± 0.02
p-xylene	2.17[h]	1.25 ± 0.05

[a]At 25 °C and 1 atm. [b]Ref 49. [c]Ref 50. [d]Ref 51. [e]Ref 52. [f]Ref 53. [g]Ref 54. [h]Ref 55. [i]Ref 56.

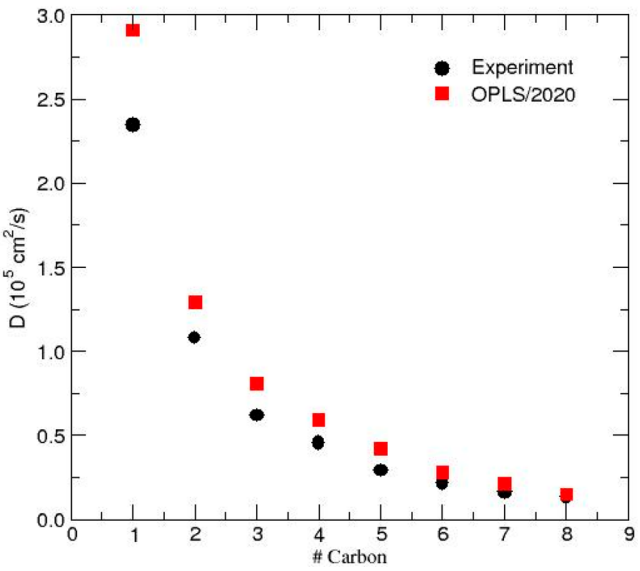

Figure 4. Self-diffusion coefficients of liquid primary alcohols as a function of chain length. For molecules with multiple experimental data sets, the average is used.

alkanes.[12] For the smallest ones, the computed diffusion is a little too high, but then, the computed and experimental values are in close agreement for the larger ones. For benzene, toluene, ethylbenzene, and *p*-xylene, the computed diffusion constants decline. This seems consistent with their increasing heats of vaporization (Table 5), which provide a measure of the average strength of the intermolecular interactions. Another MD study for liquid benzene, toluene, and *p*-xylene with a different Lennard-Jones plus Coulomb force field gave results similar to the present ones with the diffusion constant

https://doi.org/10.1021/acs.jpcb.3c06602
J. Phys. Chem. B 2024, 128, 250−262

declining from 2.19 to 1.92 to 1.49 × 10^{-5} cm^2 s^{-1}.[57] However, the available experimental data have an erratic pattern with benzene and *p*-xylene between toluene and ethylbenzene. It may also be noted that a comprehensive MD study of liquid benzene using AMBER, CHARMM, GROMOS, and OPLS-AA force fields endorsed OPLS-AA and reported a diffusion constant of (1.97 ± 0.10) × 10^{-5} cm^2 s^{-1},[58] identical to the value here for OPLS/2020. As noted above, the only change was reduction of the ε for benzene carbon atoms to 0.068 from 0.070 kcal/mol.

Free Energies of Hydration. The computed free energies of hydration for 43 molecules from the MC/FEP simulations are compared with the experimental values in Table 9 and Figure 5. The correlation of computed and experimental results is very good in Figure 5 (r^2 = 0.97), though the computed values are uniformly ca. 1 kcal/mol too positive such that the mean unsigned (mue) and mean signed errors are both 1.2 kcal/mol (Table 9). The mue can be reduced to 0.6 kcal/mol using 1.14*CM1A charges with bond-charge corrections (LBCC); however, use of those charges in simulations of pure organic liquids gives average errors of 1.40 kcal/mol for ΔH_{vap} and 0.024 g cm^{-3} for density.[20] As explained previously, the dilemma arises from the expectation that atomic charges that are optimized for computing free energies of hydration are overpolarized for representing the lower dielectric environment of organic liquids.[20] Conversely, atomic charges that are optimized for pure organic liquids are underpolarized for aqueous solutions and yield too positive free energies of hydration. The discrepancies then are expected to carry over to partitioning phenomena. With the pure-liquid optimized atomic charges, organic molecules are too hydrophobic. Thus, computed octanol/water partition coefficients should be too large and partitioning into cell membranes may be too favorable. The situation for protein−ligand binding is more complicated as the hydrophobic effect will be overstated, but electrostatic interactions including hydrogen bonding may be understated. For relative free energies of binding, significant cancellation of errors can be expected for congeneric series in view of the good correlation in Figure 5. It should be possible to overcome the problem with use of polarizable force fields, as has been demonstrated with the CHARMM-Drude force field.[60]

Considering the results in Table 9 in more detail, the error for saturated hydrocarbons does increase some with size to a maximum of 1.2−1.4 kcal/mol for cyclohexane and octane. The alkenes and 1-butyne give relatively greater errors for their size, including 1.6 kcal/mol for cyclohexene. This may arise from an underestimate of electrostatic interactions between water molecules and the polarizable π-systems. The errors for primary and secondary alcohols are less, 0.3−0.7 kcal/mol, which likely reflects the higher dielectric constants for the pure liquids yielding charges more appropriate for aqueous solutions. The 2.0 kcal/mol error for phenol may arise from the minimalist description lacking delocalization and polarizability of the π-system; with the OPLS models, the partial charges on the CH units in monosubstituted benzenes are the same as those in benzene. The errors for ethers are larger ranging from 1.6 kcal/mol for 1,2-dimethoxyethane to 2.2 kcal/mol for THF. In this case, our expectation is that additional charged sites in lone-pair-like positions on oxygen, as in TIP5P water,[61] could improve the description of hydrogen bonding.[10,62,63] In their absence, the ether oxygen atoms are too sterically shielded by the adjacent alkyl groups.

Table 9. Free Energies of Hydration (kcal/mol) at 25 °C and 1 atm[a]

Molecule	ΔG_{hyd}, TIP4P[b]	ΔG_{hyd}, Exptl.[c]	Diff.
methane	2.595	1.99	0.605
ethane	2.767	1.83	0.937
propane	2.944	1.96	0.984
butane	3.199	2.07	1.129
2-methylpropane	3.342	2.32	1.022
pentane	3.531	2.32	1.211
hexane	3.674	2.48	1.194
3-methylpentane	3.423	2.51	0.913
cyclohexane	2.605	1.23	1.375
heptane	3.852	2.67	1.182
octane	4.131	2.88	1.251
propene	2.428	1.32	1.108
2-methylpropene	2.714	1.16	1.554
1-butene	2.559	1.38	1.179
2-methyl-2-butene	2.904	1.31	1.594
isoprene	2.105	0.68	1.425
hexa-1,5-diene	2.637	1.01	1.627
cyclohexene	1.940	0.37	1.570
1-butyne	1.296	−0.16	1.456
benzene	0.251	−0.86	1.111
ethylbenzene	−0.147	−0.79	0.643
chlorobenzene	0.513	−1.12	1.633
chlorobenzene-X[d]	0.327	−1.12	1.447
methanol	−4.612	−5.10	0.488
ethanol	−4.665	−5.00	0.335
propanol	−4.307	−4.85	0.543
2-propanol	−4.365	−4.74	0.375
butanol	−4.160	−4.72	0.560
2-butanol	−3.889	−4.62	0.731
pentanol	−3.872	−4.57	0.698
hexanol	−3.912	−4.40	0.488
2-methyl-2-propanol	−3.204	−4.47	1.266
1,2-ethanediol	−10.089	−9.30	−0.789
phenol	−4.557	−6.61	2.053
benzyl alcohol	−6.323	−6.62	0.297
diethyl ether	−0.197	−1.91	1.713
tetrahydrofuran	−1.258	−3.47	2.212
tetrahydropyran	−1.026	−3.12	2.094
anisole	−0.562	−2.450	1.888
1,2-dimethoxyethane	−3.226	−4.840	1.614
2-ethoxyethanol	−4.981	−6.690	1.709
propylamine	−2.978	−4.39	1.412
diethylamine	−2.723	−4.07	1.347
triethylamine	−1.327	−3.22	1.893
mean signed error	1.161		
mean unsigned error	1.197		

[a]For transfer from the gas phase to aqueous solution with 1 M standard states. [b]Computed uncertainties are ±0.2 kcal/mol. [c]Ref 59. [d]With X site for halogen bonding.

The 1.2−1.9 kcal/mol errors for *t*-butanol (2-methyl-2-propanol) and the amines may also reflect steric shielding and potential benefit of inclusion of an extra interaction site on amine nitrogen atoms.[62,63]

CONCLUSION

The OPLS-AA force field has been updated with testing for a much greater range of organic liquids than before and inclusion of results for additional functional groups. The present release

https://doi.org/10.1021/acs.jpcb.3c06602
J. Phys. Chem. B 2024, 128, 250−262

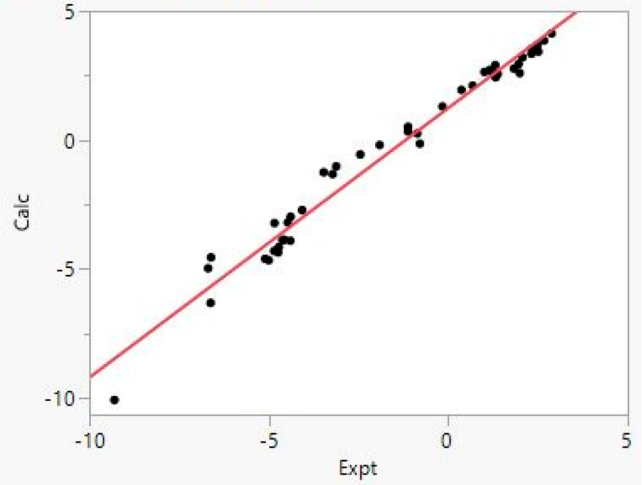

Figure 5. Experimental vs computed free energies of hydration from Table 9 in kcal/mol. The line is the best linear fit (r^2 = 0.974).

of the force field is designated as OPLS/2020. The provided files allow for complete implementation in other software and testing in comparison to the results presented here using the BOSS program. This release of OPLS-AA should not be confused with the proprietary OPLS/3 force field, which has undergone extensive, independent optimization starting from an early version of OPLS-AA.[63] Our academic efforts have been directed at providing a solid basis for gas-phase and condensed-phase simulations of a wide range of organic and biomolecular systems. Greater accuracy of the model could be achieved by an improved description of electrostatic interactions through inclusion of explicit polarization effects and additional charged sites on heteroatoms. In pressing cases like cation–π interactions and halogen bonding such additions have been made.[10−12] Broader treatments come with added expense in execution and after much effort in parametrization and testing.[1−5]

■ ASSOCIATED CONTENT

Data Availability Statement

The BOSS program is available for download from http://zarbi.chem.yale.edu. It provides a wide range of molecular modeling options with the OPLS all-atom and united-atom force fields and semiempirical molecular orbital calculations. Capabilities include energy minimizations, vibrational frequency calculations, conformational search, Monte Carlo simulations of pure liquids and solutions, QM/MM, and free-energy perturbation (FEP) calculations. It contains files with the complete force field parameters and input *Z*-matrices for ca. 3000 molecules.

Supporting Information

The Supporting Information is available free of charge at https://pubs.acs.org/doi/10.1021/acs.jpcb.3c06602.

The full list of OPLS atom types, tables of force field parameters for hydrocarbons, and details on the MD simulations (PDF)

OPLS all-atom non-bonded and torsional parameters for organic molecules, ions, peptides, and nucleic acids (TXT)

OPLS all-atom bond stretching and angle bending parameters (TXT)

■ AUTHOR INFORMATION

Corresponding Author

William L. Jorgensen − *Department of Chemistry, Yale University, New Haven, Connecticut 06520-8107, United States;* orcid.org/0000-0002-3993-9520; Email: william.jorgensen@yale.edu

Authors

Mohammad M. Ghahremanpour − *Department of Chemistry, Yale University, New Haven, Connecticut 06520-8107, United States;* orcid.org/0000-0002-1129-6041

Anastasia Saar − *Department of Chemistry, Yale University, New Haven, Connecticut 06520-8107, United States;* orcid.org/0009-0004-2961-5073

Julian Tirado-Rives − *Department of Chemistry, Yale University, New Haven, Connecticut 06520-8107, United States;* orcid.org/0000-0001-7330-189X

Complete contact information is available at: https://pubs.acs.org/10.1021/acs.jpcb.3c06602

Notes

The authors declare no competing financial interest.

■ ACKNOWLEDGMENTS

Gratitude is expressed to the National Institutes of Health (GM032136) for support of this research.

■ REFERENCES

(1) Ponder, J. W.; Case, D. A. Force Fields for Protein Simulations. *Adv. Prot. Chem.* **2003**, *66*, 27−85.

(2) Jorgensen, W. L.; Tirado-Rives, J. Potential Energy Functions for Atomic-Level Simulations of Water and Organic and Biomolecular Systems. *Proc. Natl. Acad. Sci. U. S. A.* **2005**, *102*, 6665−6670.

(3) Riniker, S. Fixed-Charge Atomistic Force Fields for Molecular Dynamics Simulations in Condensed Phase: An Overview. *J. Chem. Info Model.* **2018**, *58*, 565−578.

(4) Nerenberg, P. S; Head-Gordon, T. New Developments in Force Fields for Biomolecular Simulations. *Curr. Opin. Struct. Biol.* **2018**, *49*, 129−138.

(5) He, X.; Walker, B.; Man, V. H.; Ren, P.; Wang, J. Recent Progress in General Force Fields for Small Molecules. *Curr. Opin. Struct. Biol.* **2022**, *72*, 187−193.

(6) Jorgensen, W. L.; Chandrasekhar, J.; Madura, J. D.; Impey, R. W.; Klein, M. L. Comparison of Simple Potential Functions for Simulating Liquid Water. *J. Chem. Phys.* **1983**, *79* (2), 926−935.

(7) Jorgensen, W. L.; Tirado-Rives, J. The OPLS Force Field for Proteins. Energy Minimizations for Crystals of Cyclic Peptides and Crambin. *J. Am. Chem. Soc.* **1988**, *110*, 1657−1666.

(8) Jorgensen, W. L.; Maxwell, D. S.; Tirado-Rives, J. Development and Testing of the OPLS All-Atom Force Field on Conformational Energetics and Properties of Organic Liquids. *J. Am. Chem. Soc.* **1996**, *118*, 11225−11236.

(9) Robertson, M. J.; Tirado-Rives, J.; Jorgensen, W. L. Improved Peptide and Protein Torsional Energetics with the OPLS-AA Force Field. *J. Chem. Theory Comput.* **2015**, *11*, 3499−3509.

(10) Jorgensen, W. L.; Schyman, P. Treatment of Halogen Bonding in the OPLS-AA Force Field: Application to Potent Anti-HIV Agents. *J. Chem. Theory Comput.* **2012**, *8*, 3895−3901.

(11) Turupcu, A.; Tirado-Rives, J.; Jorgensen, W. L. Explicit Representation of Cation-π Interactions in Force Fields with $1/r^4$ Non-bonded Terms. *J. Chem. Theory Comput.* **2020**, *16*, 7184−7194.

(12) Ghahremanpour, M. M.; Tirado-Rives, J.; Jorgensen, W. L. Refinement of the OPLS Force Field for Thermodynamics and Dynamics of Liquid Alkanes. *J. Phys. Chem. B* **2022**, *126*, 5896−5907.

(13) Kaminski, G.; Duffy, E. M.; Matsui, T.; Jorgensen, W. L. Free Energies of Hydration and Pure Liquid Properties of Hydrocarbons

from the OPLS All-Atom Model. *J. Phys. Chem.* **1994**, *98*, 13077−13082.
(14) Thomas, L. L.; Christakis, T. J.; Jorgensen, W. L. Conformation of Alkanes in the Gas Phase and Pure Liquids. *J. Phys. Chem. B* **2006**, *110*, 21198−21204.
(15) Jorgensen, W. L.; Tirado-Rives, J. Molecular Modeling of Organic and Biomolecular Systems Using BOSS and MCPRO. *J. Comput. Chem.* **2005**, *26*, 1689−1700.
(16) Pronk, S.; Páll, S.; Schulz, R.; Larsson, P.; Bjelkmar, P.; Apostolov, R.; Shirts, M. R.; Smith, J. C.; Kasson, P. M.; van der Spoel, D.; Hess, B.; Lindahl, E. GROMACS 4.5: A High-Throughput and Highly Parallel Open Source Molecular Simulation Toolkit. *Bioinformatics* **2013**, *29*, 845−854.
(17) Straatsma, T. P.; Berendsen, H. J. C.; Postma, J. P. M. Free Energy of Hydrophobic Hydration: A Molecular Dynamics Study of Noble Gases in Water. *J. Chem. Phys.* **1986**, *85*, 6720−6727.
(18) Jorgensen, W. L.; Blake, J. F.; Buckner, J. K. Free Energy of TIP4P water amd the Free Energies of Hydration of CH_4 and Cl^- from Statistical Perturbation Theory. *Chem. Phys.* **1989**, *129*, 193−200.
(19) Mobley, D. L.; Bayly, C. I.; Cooper, M. D.; Shirts, M. R.; Dill, K. A. Small Molecule Free Energies of Hydration in Explicit Solvent: An Extensive Test of Fixed-Charge Atomistic Simulations. *J. Chem. Theory Comput.* **2009**, *5*, 350−358.
(20) Dodda, L. S.; Vilseck, J. Z.; Tirado-Rives, J.; Jorgensen, W. L. 1.14*CM1A-LBCC: Localized Bond-Charge Corrected CM1A Charges for Condensed-Phase Simulations. *J. Phys. Chem. B* **2017**, *121*, 3864−3870.
(21) Jorgensen, W. L.; Chandrasekhar, J.; Madura, J. D.; Impey, R. W.; Klein, M. L. Comparison of Simple Potential Functions for Simulating Liquid Water. *J. Chem. Phys.* **1983**, *79*, 926−935.
(22) Cabeza de Vaca, I.; Zarzuela, R.; Tirado-Rives, J.; Jorgensen, W. L. Robust FEP Protocols for Creating Molecules in Solution. *J. Chem. Theory Comput.* **2019**, *15*, 3941−3948.
(23) Dahlgren, M. K.; Schyman, P.; Tirado-Rives, J.; Jorgensen, W. L. Characterization of Biaryl Torsional Energetics and Its Treatment in OPLS All-Atom Force Fields. *J. Chem. Info. Model.* **2013**, *53*, 1191−1199.
(24) St.-Amant, A.; Cornell, W. D.; Kollman, P. A.; Halgren, T. A. Calculation of Molecular Geometries, Relative Conformational Energies, Dipole Moments, and Molecular Electrostatic Potential Fitted Charges of Small Organic Molecules of Biochemical Interest by Density Functional Theory. *J. Comput. Chem.* **1995**, *16*, 1483−1506.
(25) Ohlinger, W. S.; Deppmeier, B. J.; Hehre, W. J. Efficient Calculation of Heats of Formation. *J. Phys. Chem. A* **2009**, *113*, 2165−2175.
(26) Rogers, D. W.; von Voithenberg, H.; Allinger, N. L. Heats of Hydrogenation of the Cis and Trans Isomers of Cyclooctene. *J. Org. Chem.* **1978**, *43*, 360−361.
(27) Schmidt, M. W.; Truong, P. N.; Gordon, M. S. π-Bond Strengths in the Second and Third Periods. *J. Am. Chem. Soc.* **1987**, *109*, 5217−5227.
(28) Karpfen, A.; Choi, C. H.; Kertesz, M. Single-Bond Torsional Potentials in Conjugated Systems: A Comparison of Ab Initio and Density Functional Results. *J. Phys. Chem. A* **1997**, *101*, 7426−7433.
(29) Caminati, W.; Damiani, D.; Corbelli, G.; Velino, B.; Bock, C. W. Microwave Spectrum and Ab Initio Calculations of Ethylbenzene: Potential Energy Surface of the Ethyl Group Torsion. *Mol. Phys.* **1991**, *74*, 885−895.
(30) Kirschner, K. N.; Heiden, W.; Reith, D. Small Alcohols Revisited: CCSD(T) Relative Potential Energies for the Minima, First- and Second-Order Saddle Points, and Torsion-Coupled Surfaces. *ACS Omega* **2018**, *3*, 419−432.
(31) Cheng, Y.-L.; Chen, H.-Y.; Takahashi, K. Theoretical Calculation of the OH Vibrational Overtone Spectra of 1-*n* Alkane Diols (n = 2−4): Origin of Disappearing Hydrogen-Bonded OH Peak. *J. Phys. Chem. A* **2011**, *115*, 5641−5653.
(32) Tsuzuki, S.; Houjou, H.; Nagawa, Y.; Hiratani, K. High-Level ab initio Calculations of Torsional Potential of Phenol, Anisole, and *o*-Hydroxyanisole: Effects of Intramolecular Hydrogen Bond. *J. Phys. Chem. A* **2000**, *104*, 1332−136.
(33) DeTar, D. F. Thermochemical Values of Oxygen Containing Compounds form Ab Initio Calculations. 1. Enthalpies of Formation of Ethers and Alcohols. *J. Phys. Chem. A* **1999**, *103*, 7055−7068.
(34) Wiberg, K. B.; Murcko, M. A. Rotational Barriers. 4. Dimethoxymethane. The Anomeric Effect Revisited. *J. Am. Chem. Soc.* **1989**, *111*, 4821−4828.
(35) Wiberg, K. B.; Rablen, P. R. Methoxymethane C-O Bond Strengths: Do Their Changes Result from Hyperconjugation or Polar Effects? *J. Phys. Chem. A* **2018**, *122*, 6021−6025.
(36) Woodcock, H. L.; Moran, D.; Pastor, R. W.; MacKerell, A. D., Jr.; Brooks, B. B. Ab Initio Modeling of Glycosyl Torsions and Anomeric Effects in a Model Carbohydrate: E-Ethoxy Tetrahydropyran. *Biophys. J.* **2007**, *93*, 1−10.
(37) Wiberg, K. B.; Marquez, M. The Energy Components of the Anomeric Effect for 2-Methoxytetrahydropyran. An Experimental Comparison of the Gas Phase and Solutions. *J. Am. Chem. Soc.* **1994**, *116*, 2197−2198.
(38) Murcko, M. A.; DiPaola, R. A. Ab Initio Molecular Orbital Conformational Analysis of Prototypical Organic Systems. 1. Ethylene Glycol and 1, 2-Dimethoxyethane. *J. Am. Chem. Soc.* **1992**, *114*, 10010−10018.
(39) Sharapa, D. I.; Genaev, A.; Cavallo, L.; Minenkov, Y. A Robust and Cost-efficient Scheme for Accurate Conformational Energies of Organic Molecules. *ChemPhysChem* **2019**, *20*, 92−102.
(40) Feller, D.; Craig, N. C. High Level Ab Initio Energies and Structure for the Rotamers of 1,3-Butadiene. *J. Phys. Chem. A* **2009**, *113*, 1601−1607.
(41) Jorgensen, W. L.; Morales de Tirado, P. I.; Severance, D. L. Monte Carlo Results for the Effect of Solvation on the Anomeric Equilibrium for 2-Methoxytetrahydropyran. *J. Am. Chem. Soc.* **1994**, *116*, 2199−2200.
(42) Riddick, J. A.; Bunger, W. B.; Sakano, T. K. *Techniques of Chemistry.2: Organic Solvents. Physical Properties and Methods of Purification*, 4th ed.; John Wiley & Sons, Inc.: 1986; Vol. 2.
(43) Rego, T.; Silva, G. M. C.; Goldmann, M.; Filipe, E. J. M.; Morgado, P. Optimized All-atom Force Field for Alkynes within the OPLS-AA Framework. *Fluid Phase Equilib.* **2022**, *554*, 113314.
(44) Jorgensen, W. L.; Severance, D. L. Aromatic-Aromatic Interactions: Free Energy Profiles for the Benzene Dimer in Water, Chloroform, and Liquid Benzene. *J. Am. Chem. Soc.* **1990**, *112*, 4768−4774.
(45) Jorgensen, W. L. Optimized Intermolecular Potential Functions for Liquid Alcohols. *J. Phys. Chem.* **1986**, *90*, 1276−1284.
(46) Jorgensen, W. L.; Laird, E. R.; Nguyen, T. B.; Tirado-Rives, J. Monte Carlo Simulations of Pure Liquid Substituted Benzenes with OPLS Potential Functions. *J. Comput. Chem.* **1993**, *14*, 206−215.
(47) Rizzo, R. C.; Jorgensen, W. L. OPLS All-Atom Model for Amines: Resolution of the Amine Hydration Problem. *J. Am. Chem. Soc.* **1999**, *121*, 4827−4836.
(48) Antón, V.; Munoz-Embid, J.; Artal, M.; Lafuente, C. Experimental and Modeled Volumatric Behavior of Linear and Branched Ethers. *Fluid Phase Equilib.* **2016**, *417*, 7−18.
(49) Partington, J. R.; Hudson, R. F.; Bagnall, K. W. Self-diffusion of Aliphatic Alcohols. *Nature* **1952**, *169*, 583−584.
(50) Pratt, K. C.; Wakeham, W. A. Self-Diffusion in Water and Monohydric Alcohols. *J. Chem. Soc. Faraday Trans. 2* **1977**, *73*, 997−1002.
(51) Tofts, P. S.; Lloyd, D.; Clark, C. A.; Barker, G. J.; Parker, G. J. M.; McConville, P.; Baldock, C.; Pope, J. M. Test Liquids for Quantitative MRI Measurements of Self-diffusion Coefficient in Vivo. *Magn. Reson. Med.* **2000**, *43*, 368−374.
(52) McCall, D. W.; Douglass, D. C. Self-Diffusion in the Primary Alcohols. *J. Chem. Phys.* **1960**, *32*, 1876−1877.
(53) Iwahashi, M.; Ohbu, Y.; Kato, T.; Suzuki, Y.; Yamauchi, K.; Yamaguchi, Y.; Muramatsu, M. The Dynamical Structure of Normal Alcohols in Their Liquids as Determined by the Viscosity and Self-Diffusion Measurements. *Bull. Chem. Soc. Jpn.* **1986**, *59*, 3771−3774.

https://doi.org/10.1021/acs.jpcb.3c06602
J. Phys. Chem. B 2024, 128, 250−262

(54) Holz, M.; Heil, S. R.; Sacco, A. Temperature-dependent Self-diffusion Coefficients of Water and Six Selected Molecular Liquids for Calibration in Accurate 1H NMR PFG Measurements. *Phys. Chem. Chem. Phys.* **2000**, *2*, 4740−4742.
(55) Lindman, B.; Stilbs, P.; Moseley, M. E. Fourier Transform NMR Self-Diffusion and Microemulsion Structure. *J. Colloid Interface Sci.* **1981**, *83*, 569−582.
(56) Mutzenhardt, P.; Canet, D. Behavior of Longitudinal Spin Orders in NMR Measurements of Self-Diffusion Coefficients Using Radiofrequency Field Gradients. *J. Chem. Phys.* **1996**, *105*, 4405−4411.
(57) Kim, J. A.; Lee, S. H. Molecular Dynamics Simulations Studies of Benzene, Toluene, and *p*-Xylene in a Canonical Ensemble. *Bull. Korean Chem. Soc.* **2002**, *23*, 441−446.
(58) Fu, C.-F.; Tian, S. X. A Comparative Study for Molecular Dynamics Simulations of Liquid Benzene. *J. Chem. Theory. Comput.* **2011**, *7*, 2240−2252.
(59) Mobley, D. L.; Guthrie, J. P. FreeSolv: A Database of Experimental and Calculated Hydration Free Energies, with Input Files. *J. Comput. Aided Mol. Des.* **2014**, *28*, 711−720.
(60) Rupakheti, C. R.; MacKerell, A. D., Jr.; Roux, B. Global Optimization of the Lennard-Jones Parameters for the Drude Polarizable Force Field. *J. Chem. Theory. Comput.* **2021**, *17*, 7085−7095.
(61) Mahoney, M. W.; Jorgensen, W. L. A Five-Site Model for Liquid Water and the Reproduction of the Density Anomaly by Rigid, Nonpolarizable Potential Functions. *J. Chem. Phys.* **2000**, *112*, 8910−8922.
(62) Dixon, R. W.; Kollman, P. A. Advancing Beyond the Atom-Centered Model in Additive and Non-Additive Molecular Mechanics. *J. Comput. Chem.* **1997**, *18*, 1632−1646.
(63) Harder, E.; Damm, W.; Maple, J.; Wu, C.; Reboul, M.; Xiang, J. Y.; Wang, L.; Lupyan, D.; Dahlgren, M. K.; Knight, J. L.; et al. OPLS3: A Force Field Providing Broad Coverage of Drug-like Small Molecules and Proteins. *J. Chem. Theory Comput.* **2016**, *12*, 281−296.

https://doi.org/10.1021/acs.jpcb.3c06602
J. Phys. Chem. B 2024, 128, 250−262